Am J Cancer Res 2017;7(12):2422-2437
www.ajcr.us /ISSN:2156-6976/ajcr0064643

Original Article

Loss of ACVRIB leads to increased squamous cell carcinoma aggressiveness through alterations in cell-cell and cell-matrix adhesion proteins

Holli A Loomans[1,2], Shanna A Arnold[3,4], Kate Hebron[1], Chase J Taylor[3,4], Andries Zijlstra[1,4], Claudia D Andl[1,5]

[1]Department of Cancer Biology, Vanderbilt University, Nashville, TN, USA; [2]Cancer Prevention Fellowship Program, Division of Cancer Prevention, National Cancer Institute, Bethesda, MD, USA; [3]Department of Veterans Affairs, Tennessee Valley Healthcare System, Nashville, TN, USA; [4]Department of Pathology, Microbiology, and Immunology, Vanderbilt University Medical Center, Nashville, TN, USA; [5]Burnett School of Biomedical Sciences, College of Medicine, University of Central Florida, Orlando, FL, USA

Received August 29, 2017; Accepted September 7, 2017; Epub December 1, 2017; Published December 15, 2017

Abstract: Squamous cell carcinomas of the head and neck (HNSCC) and esophagus (ESCC) pose a global public health issue due to high mortality rates. Unfortunately, little progress has been made in improving patient outcomes. This is partially a result of a lack of understanding the mechanisms that drive SCC progression. Recently, Activin A signaling has been implicated in a number of cancers, yet the role of this pathway in SCC remains poorly understood. We have previously discovered that the Activin A ligand acts as a tumor suppressor when epithelial Activin receptor type IB (ACVRIB) is intact; however, this effect is lost upon ACVRIB downregulation. In the present study, we investigated the function of ACVRIB in the regulation of SCC. Using CRISPR/Cas9-mediated ACVRIB-knockout and knockdown using siRNA, we found an increased capacity to proliferate, migrate, and invade upon ACRIB loss, as ACVRIB-KO cells exhibited an altered cytoskeleton and aberrant expression of E-cadherin and integrins. Based on chemical inhibitor studies, our data suggests that these effects are mediated through ACVRIB-independent signaling via downstream activation of Smad1/5/8 and MEK/ERK. Overall, we present a novel mechanism of SCC progression upon ACVRIB loss by showing that Activin A can transduce a signal in the absence of ACVRIB.

Keywords: Activin A, squamous cell carcinoma, cytoskeleton dynamics, three-dimensional culture, adhesion

Introduction

Activin receptor-like kinases (ALKs) have been known to play a role in organism development and cancer. ALKs are a family of seven type I receptors that share high sequence homology (40-60%) and structural similarities, including an extracellular glycosylation site, transmembrane domain, and cytoplasmic tail with a serine/threonine kinase domain [1]. ALKs are the primary signal transducing receptor for the TGFβ superfamily of ligands, which includes Activins and BMPs. As there are greater than 45 ligands in the TGFβ superfamily with only seven type I receptors, there is ligand-receptor overlap [2].

ACVRIB, also known as ALK4, exemplifies the ligand-receptor overlap noted in the ALK family, as it is the primary type I receptor for several TGFβ superfamily ligands, including Activin A [3, 4]. ACVRIB is recruited by a type II receptor upon ligand binding initiating downstream phosphorylation of Smad2/3 or Smad1/5/8, which forms a complex with Smad4 and translocates to the nucleus. The Smad-dependent pathway is considered the canonical pathway, however several non-canonical pathways, such as MEK/ERK, have been implicated in connection with ligand activity [5]. Complicating our understanding of the downstream signaling activation is that phospho-Smad1/5/8, which is primarily involved in BMP signaling, can also be phosphorylated in response to Activin A stimulation [6]. This leads to the assumption that possible complexes can be formed between different combinations of type I and type II recep-

tors, as demonstrated in several recent reports [7-9].

ALKs have been found to play critical roles in both development and cancer. The essential functions of ACVRIB, in particular, has been demonstrated in morphogenesis and differentiation. This has also been exemplified in mouse models, as global knockout of *Acvr1b* results in embryonic lethality [10]. Conditional deletion of *Acvr1b* in squamous tissues showed no detriment to the oral cavity or esophagus, yet affected hair follicle cycling leading to hair loss, increased proliferation, and stunted growth [11]. The results of these different models indicate the necessity of ACVRIB for proper embryonic and post-natal development.

In addition to having a prominent role in development, altered ACVRIB has been associated with cancer progression. An example of dysregulated ACVRIB has been observed in pituitary cancer in the form of splice variants. These splice variants lack the kinase domain and are therefore unable to propagate signal [12, 13]. In pancreatic cancer, loss or genetic inactivation of ACVRIB occurs in approximately 2% of cancers [14, 15], suggesting a role for ACVRIB as a tumor suppressor. We have recently documented the loss of ACVRIB in esophageal squamous cancers, but mutations in head and neck squamous cancers have also been reported [1, 16].

Based on our previous observations that ACVRIB loss occurs in esophageal squamous cell carcinoma (ESCC), the focus of this study was to induce ACVRIB loss and analyze the subsequent functional consequences in esophageal and head and neck (HNSCC) squamous cell carcinoma. We have shown that Activin A is not only upregulated in ESCC, but that the upregulation of stromal Activin A inversely correlates with loss of epithelial ACVRIB expression across stage, suggesting that ACVRIB is responsible for mediating the tumor suppressive effects of Activin A [3]. This has been shown in a separate cohort of ESCC patient samples, where approximately 59% had upregulated *INHBA*, compared to normal tissues [17]. In both ESCC and oral squamous cell carcinoma, increased Activin A expression was associated with tumor stage, lymph node metastasis, and poor prognosis [18, 19]. Based on our previous findings in ESCC, we hypothesized that loss of ACVRIB leads to tumor progression through the regulation of adhesion and invasion. In this study, we altered ACVRIB in HNSCC and ESCC cell lines to examine the role of this type I receptor in cell migration and invasion. We found that not only do cells with reduced expression of ACVRIB demonstrate increased *in vitro* proliferation, migration, and invasion, but that this occurs through the regulation of proteins involved in cell-cell and cell-extracellular matrix (ECM) interactions. Overall, the results of this study indicate a novel role for ACVRIB in the homeostatic maintenance of the epithelial and stromal compartments.

Materials and methods

Cell culture

The HNSCC cell line OSC-19 and oral cancer-associated fibroblasts were cultured in DMEM, supplemented with 10% fetal bovine serum (FBS) and 1% penicillin and streptomycin (P/S) (Gibco, Grand Island, NY). The esophageal squamous cell carcinoma cell line KYSE520 was cultured in RPMI, supplemented with 10% FBS and 1% P/S (Gibco).

CRISPR/Cas9 cell line generation

Knockout of ACVRIB in OSC-19 cells was generated using the Genome-Wide knockout kit, purchased from Origene (Rockville, MD) and performed according to the manufacturer's protocol. Following transfection, OSC-19 cells were selected with puromycin (2 μg/ml) and single clones isolated. Clones were screened by Western blot and validated by flow cytometry.

siRNA transfection

KYSE20 cells were seeded in a 6-well plate at a density of 200,000 cells per well. The following day, cells were transfected with 10 nM ON-TARGET plus siRNA Smart Pool or non-targeting control (GE Dharmacon, Lafayette, CO) diluted with Lipofectamine RNAiMax (Life Technologies, Carlsbad, CA) in OPTI-MEM (Gibco). Cells were either trypsinized and reseeded for assays after 24 hours or harvested for RNA or protein after 48 hours.

Flow cytometry

Flow cytometry for ACVRIB expression: Flow cytometry experiments were performed by the

Vanderbilt Medical Center Flow Cytometry Shared Resource. To discern the ACVRIB-KO population, OSC-19 cells were first trypsinized, washed with 1×PBS and resuspended at 5×10^6 cells/ml in 1×PBS. In a separate tube, 100 µl of the cell suspension was transferred and ACVRIB antibody (cat. no. ab109300; Abcam, Cambridge, UK) was added to a final dilution of 1:100. Cells were incubated for 30 minutes at room temperature, then washed with 1×PBS and centrifuged. The anti-rabbit secondary antibody Alexa 647 (Life Technologies) was added at 1:1000 and incubated at room temperature for 20 minutes. Cells were washed with 1×PBS, centrifuged, and resuspended in flow cytometry buffer. Unstained cells and ACVRIB-positive cells were used to set gates.

Propidium iodide cell cycle analysis: Cell cycle analysis, determined by propridium iodide (PI) staining, was performed as follows. OSC-19 and KYSE520 cells were first trypsinized, washed with 1×PBS, and resuspended at 2×10^6 cells/ml in ice-cold 1×PBS. Following resuspension, 9 ml of ice cold 70% ethanol was added and cells were incubated at -20°C overnight. Cells were washed with cold 1×PBS, centrifuged and resuspended in 500 µl PI staining solution (0.1% Triton X-100, 2 mg RNAse A, 400 µl 500 µg/ml PI in 1×PBS) overnight at room temperature. The following day, cells were analyzed in the Vanderbilt Medical Center Flow Cytometry Shared Resource on a 5-laser BD LSRII. Cell cycle analysis is depicted using FACSDiva 8.0 software (BD Biosciences).

Western blot

Cells were plated in 6-well plates at an initial density of 200,000 cells/well. Prior to beginning treatment, cells were serum-starved overnight at 37°C. Following overnight starvation, cells were pre-treated with 250 nM DMH1 (ALK2i; Tocris, Bristol, UK) or kept in serum-free media overnight at 37°C. The next day, cells were treated with Activin A (ActA: 10 ng/ml; R&D Systems), follistatin (FST: 100 ng/ml; R&D Systems), or kept in serum-free media for 30 minutes. Cell lysates were collected and Western blots performed. Fiji for ImageJ was used to complete densiometric analysis. Expression was normalized to α-tubulin and control/no treatment conditions.

Immunofluorescence

Formalin-fixed, paraffin-embedded sections: Staining of formalin fixed paraffin-embedded sections were performed as previously described [3]. The antibodies used for immunofluorescence are listed in Supplemental Table 1.

Phalloidin: Phalloidin staining was performed using CytoPainter Phalloidin-iFluor 488 (Abcam), according to the manufacturers' instructions, and mounted with ProLong Gold Antifade with DAPI (Life Technologies).

Proliferation

EdU: ACVRIB-KO or control cells were seeded at low density (500 cells/coverslip) on 0.02% gelatin-coated coverslips in growth media. Following adherence, coverslips were washed with 1×PBS and incubated with 5 µM EdU (Abcam) in growth media. Next, cells were fixed for 30 minutes with 4% paraformaldehyde at room temperature and washed three times for five minutes each with 1×PBS. Cells were permeabilized for 30 minutes using 0.5% Triton-X 100, diluted in 1×PBS. Subsequently, cells were incubated with the EdU development cocktail (100 mM Tris-buffered saline pH 7.6, 4 mM $CuSO_4$, 5 µM sulfo-cyanine 3 azide, 100 µM sodium ascorbate). Finally, cells were rinsed with 1×PBS three times for five minutes each and mounted on slides using ProLong Gold Anti-fade with DAPI (Life Technologies). Slides were imaged on an Olympus BX61WI upright fluorescent microscope using Volocity Imaging Software (Perkin-Elmer, Waltham, MA).

Cell counting: To further investigate proliferation, cells were first seeded in 6-well plates at a density of 10,000 cells/well (day 1). At 48 hour intervals, cells were dissociated using 0.25% trypsin (Gibco) and counted using a hemacytometer and 0.4% Trypan Blue solution (Gibco). Fold-change relative to day 1 was calculated.

Magnetically attachable stencil (MAts) migration assay

MAts assays were performed as previously described [20]. Briefly, MAts were fabricated and coated with 1% pluronic solution diluted in 1×PBS. Prior to use, MAts were rinsed, sterilized under UV light, and added to a gelatin coated 12-well plate. Then, 200,000 or 250,000

cells were seeded in each well. After adherance, they were washed and serum-starved overnight. The MAts were then removed using a forceps. Images were taken upon MAts removal and at 12-hour intervals. Results were calculated using TScratch (NIH, Bethesda, MD) [20].

Boyden chamber assays

Migration: Boyden chamber assays were performed in 24-well format according to the manufacturer's instructions. Briefly, cells were trypsinized, centrifuged, and resuspended at 100,000 cells/ml. A chemoattractant (growth media or cancer-associated fibroblast conditioned media [CAF CM]) was added to the bottom chamber at 750 µl/well. 500 µl (50,000 cells) were added to the top chamber. The plates were incubated at 37°C for approximately 24 hours. The cells were then washed with 1×PBS and fixed using 100% methanol at -20°C for 10 minutes. Chambers were immediately moved to a 0.1% crystal violet solution and stained while rocking overnight. The next day, the chambers were removed from the crystal violet solution, washed with water, cleaned, and allowed to dry. When the membranes were dry, they were carefully removed with a scalpel and mounted on slides using Permount (Fisher). Slides were allowed to dry overnight before being imaged. Cells were counted, presented as number of cells per high-powered field (hpf), and data analyzed by Student's t-test.

Invasion: Boyden chamber invasion assays using Biocoat Matrigel Invasion Chambers (Corning), were performed as described above, with the exception that chambers were rehydrated with serum-free media for 2 hours at 37°C prior to cell seeding.

Oralsphere assay

Oralsphere assays were performed similarly to that described in Shrivastava *et al.* [21]. Briefly, OSC-19 cells were dissociated to single cells using 0.25% Trypsin (Gibco) and centrifuged at 1,000 g for five minutes. Cells were resuspended in growth media and added to ultralow attachment plates (Corning) at 5,000 cells/well. At day 7, cells were collected, dissociated with 0.25% Trypsin to return cells to single cell suspension, counted, and reseeded. Wells were imaged every two days, beginning at day 1. Images were analyzed using Fiji for ImageJ [22].

Organotypic reconstruct cultures

Organotypic cultures (OTC) were performed as previously described [23]. In addition to the referenced protocol, OTCs were treated with several recombinant proteins or chemical inhibitors beginning at day 7 of the OTC protocol. Treatments were refreshed every two days during the treatment period.

HNSCC tissue microarray

HNSCC tissue microarrays (TMA) were purchased from US Biomax (cat. no. HN803c, Rockville, MD). After staining, TMAs were scanned for digital analysis. Exposure time and area analyzed were equivalent for all cores on the same slide. Cores were quantified using the "Measure Stained Area Fluorescence" algorithm as part of the Leica Microsystems Tissue IA version 4.0.6 (Buffalo Grove, IL). Fluorescence area was measured in μm^2. Analysis of the tissue sections were performed as previously described [3].

Biostatistical analysis

Experimental results were analyzed using Student's *t*-test or one-way ANOVA and expressed as the mean +/- standard deviation. Statistical analysis of the *in vitro* experiments was performed in Prism 6.0 (GraphPad, San Diego, CA). HNSCC TMA data was analyzed using SPSS (IBM, Armonk, NY).

Results

Loss of ACVRIB results in a proliferative phenotype in a HNSCC cell line

As discussed above, loss of ACVRIB has been documented in a variety of cancers and has therefore been flagged as a putative tumor suppressor [3, 14, 16, 24, 25]. However, the functional effects of loss of ACVRIB have yet to be fully elucidated. To investigate the consequences of ACVRIB loss, we utilized the CRISPR/Cas9 model to knockout ACVRIB in the HNSCC cell line OSC-19. Following validation of ACVRIB loss (ACVRIB-KO) by flow cytometry, immunofluorescence, and Western blot (Supplemental Figure 1), we examined the proliferative capabilities of

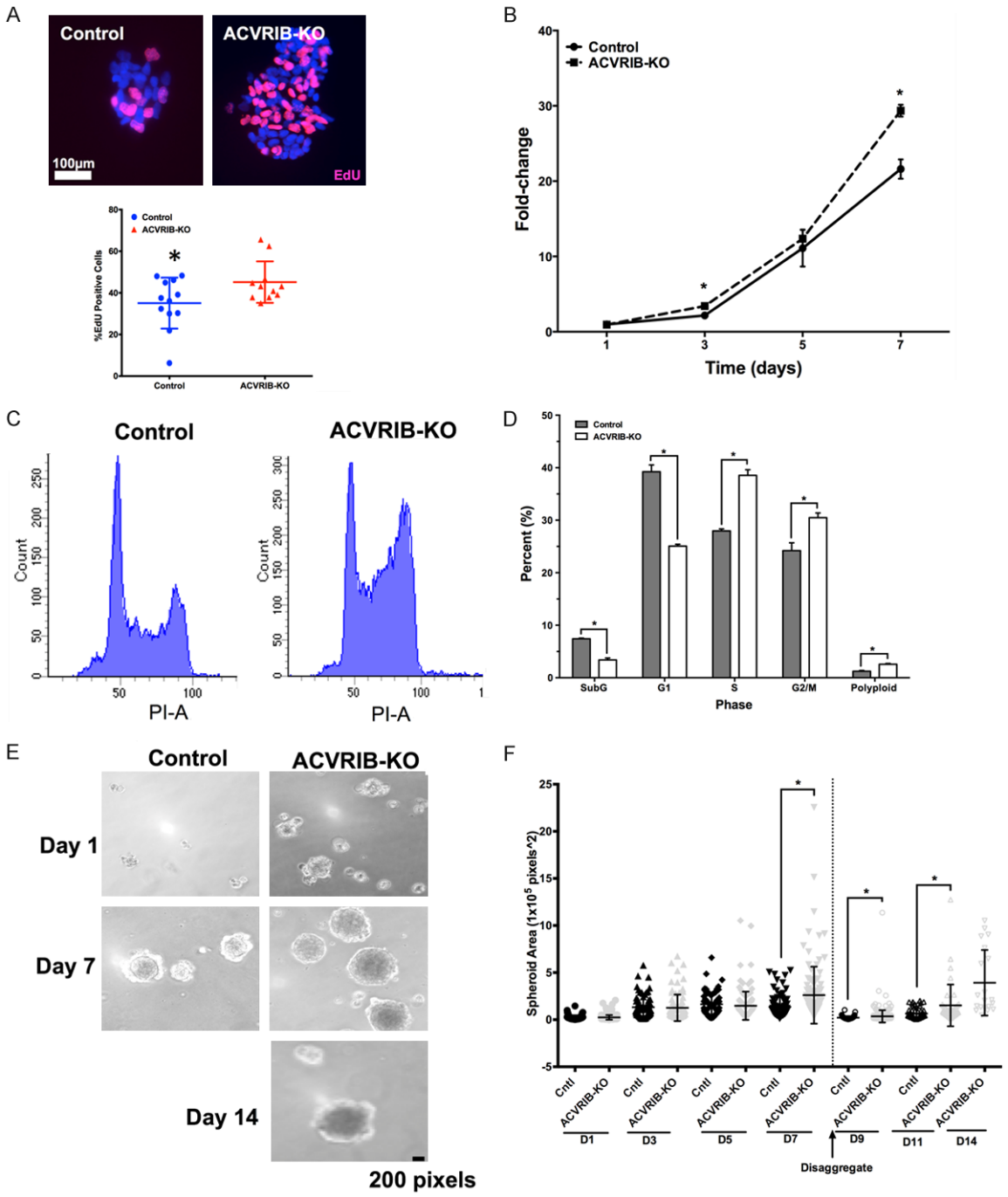

Figure 1. ACVRIB-KO cells exhibit increased proliferation and self-renewal. Proliferation of ACVRIB-KO and control OSC-19 cells was examined by several methods. A. Staining of OSC-19 cells demonstrated increased incorporation of EdU into ACVRIB-KO cells, compared to control. B. Validation of EdU staining was performed by cell counting, using 0.25% Trypan Blue to exclude dead cells. By day three of culture, ACVRIB-KO cells showed substantially increased proliferation compared to control. C. Cell cycle analysis by propidium iodide (PI) staining in flow cytometry. D. Statistical analysis of flow cytometric cell cycle analysis. ACVRIB-KO cells had significantly less cells in G1, while more were observed S and G2/M; Student's t-test, $^*p<0.05$. E. Oralspheres were grown over the course of 14 days, with disssociation on day 7 with 0.25% Trypsin and reseeding. Upon reseeding, only ACVRIB-KO cells survived to day 14. F. Oralspheres were imaged and measured using Fiji for ImageJ. Conditions were compared by Student's *t*-test, $^*p<0.05$.

these cells, as a well-established function of Activin A-ACVRIB is growth inhibition [26]. Using complementary approaches to determine proliferation of ACVRIB-KO cells (5-ethynyl-2'-de-

oxyuridine (EdU) incorporation and cell counting), we observed increased proliferation of ACVRIB-KO cells compared to controls (**Figure 1A**, **1B**). We additionally performed cell cycle analysis by propidium iodide (PI) staining in flow cytometry and found a significantly decreased number of cells in G1 and an increased number of cells in S and G2/M phases, confirming the proliferative phenotype observed prior (**Figure 1C**, **1D**). Similar results were obtained in the KYSE520 cells with knockdown of ACVRIB with siRNA (Supplemental Figure 2). These results suggest that loss of ACVRIB allows for unregulated SCC proliferation and clonal expansion.

We continued our investigation in an oralsphere assay, where cell survival, self-renewal, and cell-cell adhesion is tested through anchorage independence. On day 1, similarly sized oralspheres between conditions were observed, however, after seven days ACVRIB-KO cells formed significantly larger oralspheres (**Figure 1E**, **1F**). Following dissociation of the oralspheres, ACVRIB-KO cells were able to recover and re-establish spheres. By day 14, only the ACVRIB-KO cells survived in anchorage-independent conditions (**Figure 1E**, **1F**). Therefore, this assay suggests that loss of ACVRIB enhances the ability of HNSCC cells to survive through self-renewal and participation in cell-cell adhesion.

Cell motility is increased in the absence of ACVRIB

Several studies have suggested that Activin A signaling can drive migration and invasion; for example, Yoshinaga and colleagues showed that ESCC cell lines overexpressing Activin A had increased *in vivo* tumorigenicity compared to mock transfected cells [27]. However, this and other studies focused on the upstream action of the Activin A ligand and did not define the signaling complex required for the observed effect. As our previous study showed an inverse correlation of increased Activin A expression and decreased expression of ACVRIB, we aimed to determine if this could be a mechanism to explain the aforementioned studies. First, using magnetically attachable stencils (MAts) on gelatin-coated plates, we examined how loss of ACVRIB affects directional migration [20]. ACVRIB-KO cells had significantly less open area in the MAts void after 12 hours compared to control cells (**Figure 2A**, **2B**). After 24 hours, the void was closed for both ACVRIB-KO cells and controls (data not shown). Similar to OSC-19, downregulation of ACVRIB in KYSE520 cells by siRNA (siACVRIB) significantly decreased the open void area after 12 and 24 hours, compared to controls (siNT) (Supplemental Figure 3A, 3B).

Next, we tested chemotactic migration of ACVRIB-KO and control OSC-19 cells using Boyden chambers in the presence of growth media and oral cancer-associated fibroblast conditioned media (CAF CM) (**Figure 2C**). ACVRIB-KO cells showed increased ability to migrate and invade towards both growth media and CAF CM (**Figure 2D**). Interestingly, CAF CM was a more potent chemoattractant for the ACVRIB-KO and control cells, suggesting a role for epithelial-mesenchymal crosstalk in this process [28]. Although the siACVRIB KYSE520 cells did not increase migration in the presence of CAF CM compared to control, they did exhibit a more invasive phenotype when CAF CM was used as a chemoattractant (Supplemental Figure 3C, 3D). Overall, this data suggests that loss of ACVRIB function enhances the ability of SCCs to migrate and invade.

As we observed increased migration and invasion upon ACVRIB loss, we decided to further examine cell morphology and structure. Control cells grew with a cobblestone-like morphology characteristic of squamous epithelia as seen by bright-field microscopy (**Figure 3A**, **3B**). Upon loss of ACVRIB, OSC-19 cells formed small clusters with lamellopodial projections (**Figure 3C**, **3D**, arrowheads). This led us to examine the composition of the ACVRIB-KO actin cytoskeleton by immunofluorescent phalloidin. Compared to control cells, which showed high actin density along the cell surface, ACVRIB-KO cells had bundled actin projections as seen in filopodia (**Figure 2E-H**). This data suggests that ACVRIB is involved in actin cytoskeletal structure and/or dynamics, which impacts cell motility.

ACVRIB loss dysregulated cell-cell and cell-ECM protein expression in three-dimensional culture

To assess the functional consequences of ACVRIB loss in a complex physiological context, we grew OSC-19 ACVRIB-KO cells in three-

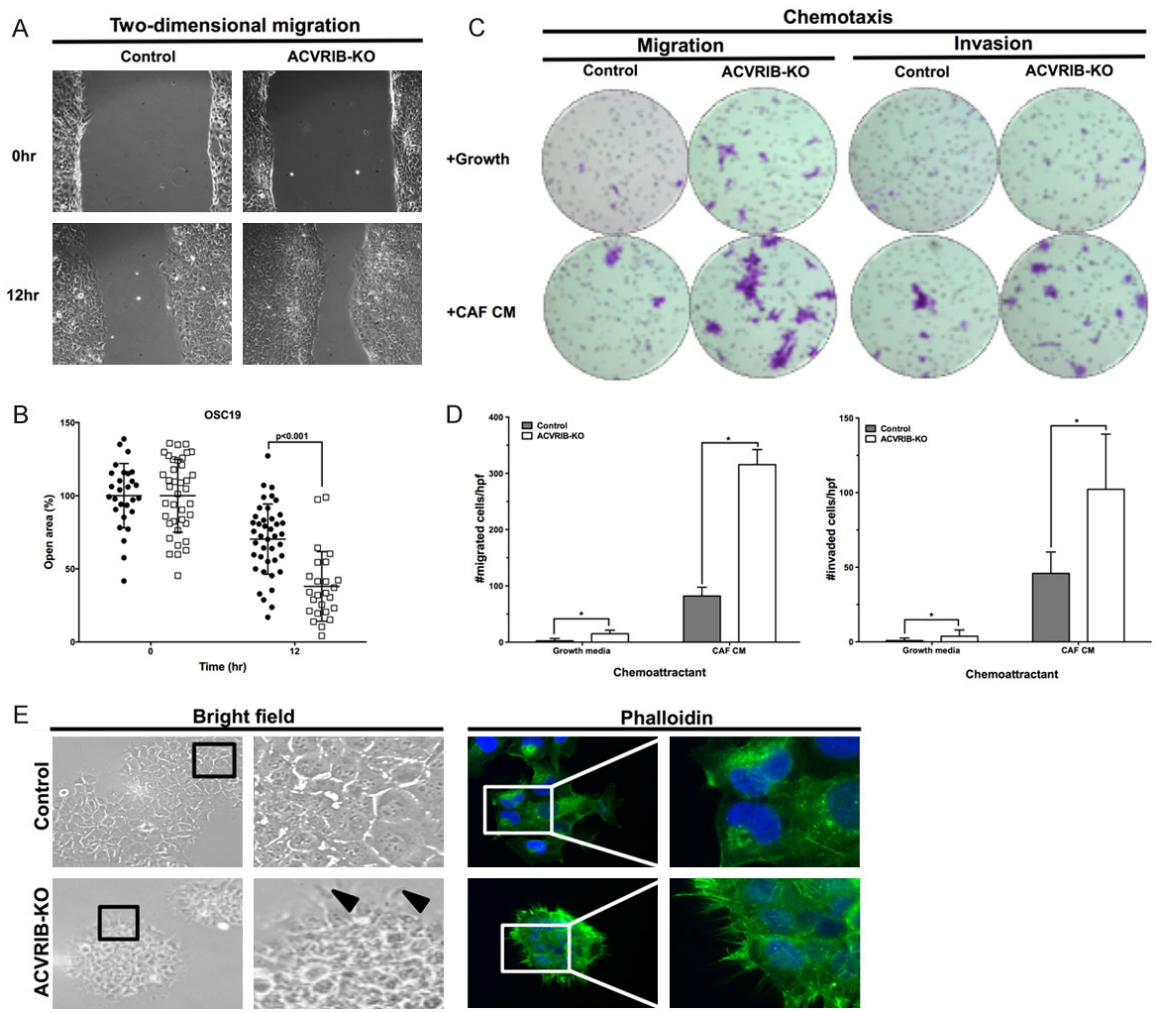

Figure 2. Migration and invasion capabilities of OSC-19 cells are enhanced with ACVRIB loss. A. Directional migration investigated using MAts assay for cells seeded on a gelatin-coated surface was assessed over the course of 12 hours. Data show enhanced migration in ACVRIB-KO cells (right), compared to control (left). B. Graphic depiction of the data points shows ACVRIB-KO cells significantly reduced the open area of the MAts by 12 hours, compared to control (Student's *t*-test, $^{*}p<0.001$). C. ACVRIB-KO cells demonstrated increased chemotactic migration (left) and invasion (right), using growth and cancer-associated conditioned media (CAF CM) as chemoattractant in Boyden chamber assays. D. Statistical analysis for cell counts per high-powered field (hpf) of Boyden no capitalization of Chamber Migration (left) and Invasion (right) assays using Student's *t*-test, $^{*}p<0.05$. E. Control OSC-19 cells have a characteristic squamous cell morphology showing a cobblestone structure using brightfield microscopy (left). Upon CRISPR/cas9-mediated deletion of ACVRIB, OSC-19 cells maintain cobblestone-like, but develop filopodia at the outer edge of the cluster (arrowheads). Phalloidin (green, right) binds to the actin filament bundles labeling filopdia. Higher magnifcation of corresponding boxed areas is shown to the right of each image.

dimensional organotypic reconstruct cultures (OTC). Hematoxylin and eosin (H&E) staining showed increased epithelial invasion into the underlying stroma (**Figure 3A**, **3B**, insets) confirming the observation of increased cell mobility upon loss of ACVRIB in two-dimensional culture (**Figure 2C**, **2D**; Supplemental Figure 3C, 3D).

Next, we performed immunofluorescence staining to assess potential changes in the expression and/or localization of cell-cell and cell-ECM adhesion proteins in the OTC. Integrins are a main group of cell surface proteins responsible for adherence to the ECM. Laboratory and clinical evidence has suggested alterations in integrin expression occur in SCC. One group found reduced expression of integrin β1, commonly used as a stem cell marker, correlated with lymph node metastasis in oral SCC, however, a separate study found increased expression of β1 in oral SCC compared to neoplastic

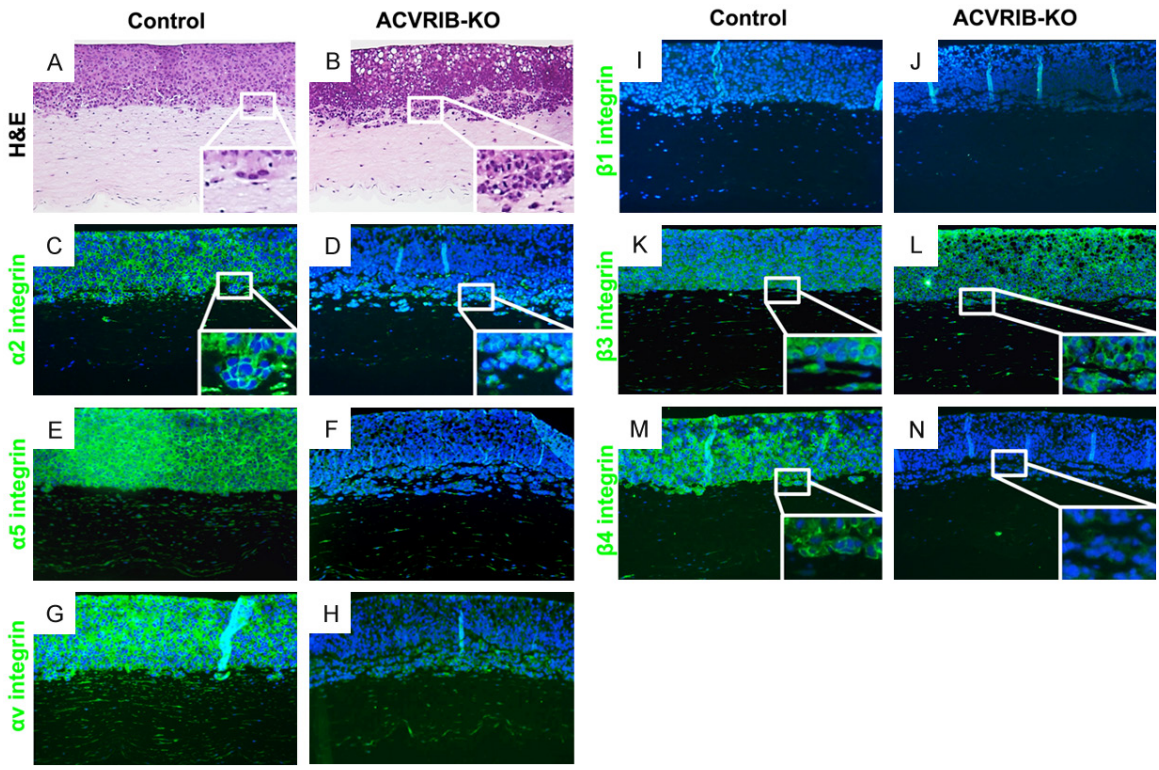

Figure 3. Loss of ACVRIB enhances cell invasion and alters integrin expression profile in three-dimensional organotypic culture. Hematoxylin and eosin (H&E) staining of (A) control and (B) ACVRIB-KO cultures showed increased invasion loss into the underlying matrix upon ACVRIB, see insert. Immunofluorescence staining for integrins α2 (C, D), α5 (E, F), αv (G, H) and β4 (M, N) showed decreased signal intensity in the more invasive ACVRIB-KO cultures. β1 integrin (I, J) remains unchanged, while β3 (K, L) was increased.

oral mucosa [29, 30]. In an additional study, Stojanovic and colleagues found several additional integrin pairings, such as αvβ3 and αvβ5, upregulated, suggesting that these proteins may help confer therapeutic resistance in oral SCC [31]. Therefore, we decided to examine a panel of integrins thought to be involved in SCC progression. We found loss of expression of several integrins (α2, α5, αv, and β4 (**Figure 3C-H**, **3M**, **3N**, insets)) in ACVRIB-KO OSC-19 cells by immunofluorescence. Integrin β1 was expressed at low to undetectable levels in control and ACVRIB-KO cells (**Figure 3I**, **3J**). There was no change in expression of integrin β3 (**Figure 3K**, **3L**, insets). The downregulation of α2, α5, αv, and β4 integrin in ACVRIB-KO cells suggests that ACVRIB may regulate not only these proteins which are major cell surface receptors involved in mediating cellular response to ECM binding, but also cytoskeleton stability, as integrins are intimately linked to cytoskeleton assembly.

Differentiation of OSC-19 cells correlates with an invasive phenotype

Integrin expression and epithelial cell differentiation are closely tied processes [32, 33]. As we observed drastic alterations in integrin expression in OSC-19 cells with loss of ACVRIB, we investigated if the differentiation status of these cells was modified. Downregulation of E-cadherin expression and cytokeratins have been associated with dedifferentiation of squamous epithelial cells. For example, downregulated E-cadherin expression has been noted in several HNSCC and ESCC studies, and found to be associated with poor prognosis [34-36]. ACVRIB-KO cells showed a substantial downregulation, but not complete loss, of E-cadherin (**Figure 4C**, **4D**, insets). Within the ACVRIB-KO invasive cells, a limited signal for E-cadherin expression was detected at the cell-cell junctions. Overall, the intensity was reduced compared to control. Vimentin was used to discern the stroma from the epithelium.

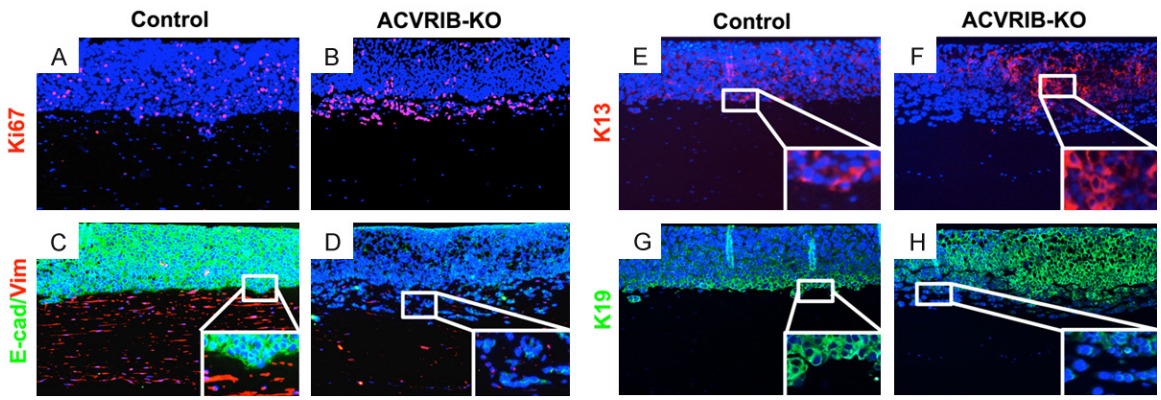

Figure 4. Loss of ACVRIB impacts squamous cell proliferation and differentiation. ACVRIB-KO cells expressed a different keratin signature compared to controls. (A, B) Ki67, (C, D) E-cadherin/E-cad and vimentin/Vim, (E, F) cytokeratin 13/K13, (G, H) cytokeratin 19/K19.

To further examine the differentiation status of these squamous cells, we decided to focus on cytokeratin 13 (K13), a marker of differentiated squamous epithelial cells, and cytokeratin 19 (K19), a marker of dedifferentiated squamous epithelial cells. K13 downregulation and K19 upregulation by both RNA and protein has been noted in esophageal and oral SCC [37, 38]. The control cells had K13 expression throughout the epithelial layer, while K13 increased in focal areas of the ACVRIB-KO squamous epithelium (**Figure 4E**, **4F**, insets). K19 expression was concentrated along the basal layer of the control cells, but highly expressed throughout the ACVRIB-KO squamous epithelium (**Figure 4G**, **4H**, insets). Cytokeratins K14, K15, and K18 were also examined and revealed no discernable differences (data not shown).

Based on the findings that ACVRIB-KO cells were highly proliferative (**Figure 2**), we also stained for Ki67 expression. Compared to the control cells, ACVRIB-KO cells had a concentrated number of proliferative cells along the invasive edge of the epithelial layer (**Figure 4A**, **4B**). This observation is intriguing, as it suggests that ACVRIB-KO cells invade and proliferate concomitantly.

In the absence of ACVRIB, Activin A can induce invasion through alternative signaling

To identify the intrinsic changes induced by the loss of ACVRIB ultimately manifesting in the observed proliferation, migration and invasion, we focused on the activation of the signaling pathway. Recent evidence has suggested that Activin A can propagate signals via other Activin type I receptors, such as BMP receptor ALK2, though ACVRIB is the primary receptor facilitating Activin A signaling. ALK2 and ACVRIB signal through distinct downstream pathways. ALK2 preferentially phosphorylates Smad1/5/8, while ACVRIB primarily phosphorylates Smad2 [10]. However, it has been suggested that crossover between Activin A-induced signaling through ACVRIB and ALK2 can occur [39]. Therefore, we aimed to determine if Activin A could signal through ALK2 as an alternate receptor in the absence of ACVRIB.

We treated ACVRIB-KO OSC-19 cells grown in OTC (**Figure 5A**, **5B**) with an ALK2 inhibitor DMH1 [40] (ALK2i, **Figure 5C**, **5I**), Activin A (ActA, **Figure 5D**, **5K**), and/or the ALK4/5/7 chemical inhibitor A83-01 [41] (**Figure 5E**, **5L**). We noted no effect of the ALK2i, ActA, or ActA/A83-01/ALK2i combination treatments on invasion (**Figure 5C**, **5D**, **5G**, **5J**, **5K**, **5N**), however, A83-01 and A83-01 in combination with ALK2i resulted in not only epithelial epithelial cell invasion into the stroma, but also a thinner stromal layer (**Figure 5E**, **5F**, **5L**, **5M**). Combination treatment with A83-01/ALK2i, also resulted in a thinner epithelial layer (**Figure 5F**, **5M**), potentially suggesting an effect of TGFβ pathway inhibition together with ACVRIB inhibition, as A83-01 additionally targets ALK5 and ALK7 (**Figure 5F**, **5M**). Particularly, the cultures treated with only ALK2i or all three treatments (ActA/A83-01/ALK2i) showed larger invasive clusters compared to the ActA only treatment (**Figure 5C**, **5G**, **5J**, **5N**).

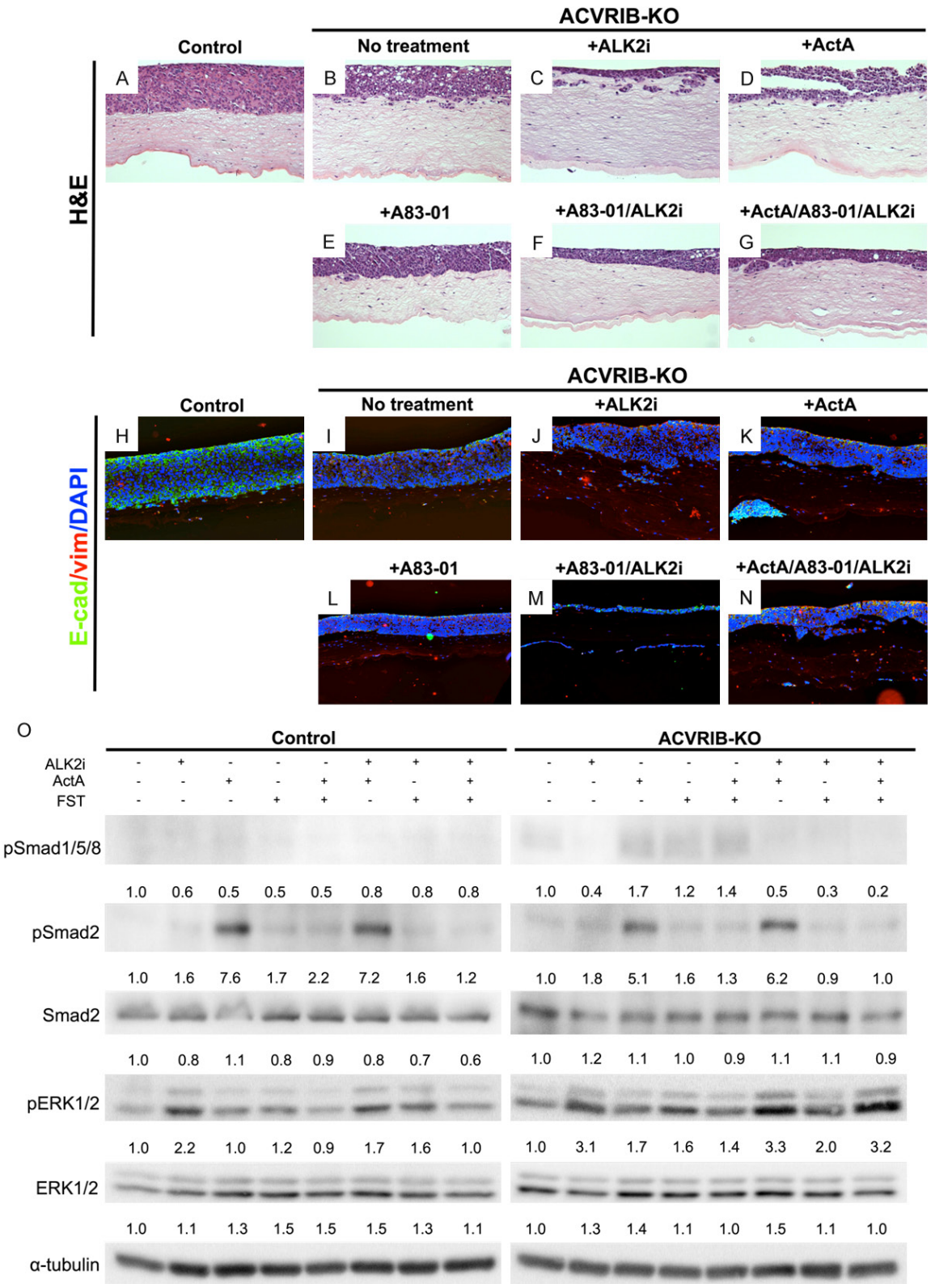

Figure 5. Chemical inhibition of Activin type I receptors alters the invasive capabilities of OSC-19 ACVRIB-KO through the regulation of Smad1/5/8 and ERK signaling. OSC-19 cells in organotypic culture (OTC) with no treatment (A, H) were used as a control for inhibition of ACVRIB-KO cells. Hematoxylin and eosin (H&E) staining of control (A) and ACVRIB-KO (B-G) OTCs, with and without treatments. Treatment conditions were as follows: (A) Control, (B) ACVRIB-

KO no treatment (No tx), (C) the ALK2/Activin receptor type IA inhibitor DMH1 (ALK2i), (D) recombinant Activin A (ActA), (E) the ALK 4/5/7 inhibitor A83-01, (F) A83-01 and ALK2i, and (G) combination ActA, A83-01, and ALK2i. (H-N) The same conditions were stained for E-cadherin (green), vimentin (red), and nuclear DAPI (blue). (O) Western blots using protein lysates harvested 30 minutes after treatments with ActA, follistatin (FST), or combination treatment to identify phosphorylation and activation of Smad (pSmad2 and pSmad1/5/8) and ERK-mediated signaling. Conditions including ALK2i were pre-treated overnight. Representative Western blots were adjusted uniformly for brightness and cropped at the appropriate molecular weight to clearly show expression of the designated protein. Western blots were quantified by densitometry using Fiji for ImageJ, normalized to α-tubulin and control. Relative expression is presented beneath each blot.

Next, we examined E-cadherin and vimentin expression by immunofluorescence. Similar to the observations described earlier, control OSC-19 cells expressed substantial levels of E-cadherin (**Figure 5H**), while ACVRIB-KO cells showed increased epithelial cell invasion and minimal E-cadherin staining (**Figure 5C**, **5D**). None of the treatments were able to restore E-cadherin expression, suggesting intrinsic alterations following ACVRIB knockout (**Figure 5J-N**). These results suggest that a balance of the TGFβ/Activin/BMP signaling pathways is required to maintain squamous epithelium integrity and limit cell invasion. Additionally, the loss of ACVRIB may upend this balance and, therefore, reroute Activin A to induce other arms of pathways or potentially signal through receptors outside of this family of receptors (**Figure 5G**, **5N**).

In order to dissect pathway activation, we next examined alterations in downstream signaling in the absence of ACVRIB. As mentioned above, ACVRIB primarily phosphorylates Smad2 to induce downstream gene transcription. However, we speculated that in the absence of ACVRIB perhaps Activin A signaling could induce signaling transduction through other downstream targets, accounting for the observed functional alterations. To explore this, we treated control or ACVRIB-KO cells *in vitro* with ALK2i, ActA, or the Activin A antagonist follistatin (FST) to block Activin A prior to receptor binding. Control cells had phosphorylated Smad2 (pSmad2) following treatment with ActA and ALK2i, however pSmad2 was blocked when ActA and FST were added together, demonstrating the efficacy of FST as an Activin A inhibitor (**Figure 5O**, left panel). Phosphorylated Smad1/5/8 (pSmad1/5/8) was unchanged between control conditions. In the ACVRIB-KO cells, ActA treatment induced pSmad2, except when treated in combination with FST, indicating that this pathway remains intact (**Figure 5O**, right panel). Interestingly, ACVRIB-KO cells had increased baseline pSmad1/5/8 compared to control cells, indicating active BMP signaling (**Figure 5O**). Upon treatment of these cells with ALK2i, pSmad1/5/8 expression was abolished, suggesting successful inhibition of BMP signaling in the presence of ActA stimulation. Therefore, we conclude from these experiments that, in the absence of ACVRIB, Activin A retains downstream activity through the Smad cascade, mediated by Smad2, and that phosphorylation of Smad1/5/8 occurs via ALK2.

Finally, we examined alterations in MEK/ERK signaling, as Activin A and ERK signaling are suggested to work together to enhance native pluoripotency and promote proliferation [42]. Phosphorylation of ERK 1/2 (pERK 1/2) was unchanged across conditions in the control cells (**Figure 5O**, left panel). ACVRIB-KO cells, however, had considerable alterations across conditions. Though all treatment conditions induced pERK 1/2 to some extent, compared to ACVRIB-KO no treatment, treatment with ALK2i/ActA or ALK2i/ActA/FST showed the highest level of phosphorylation (**Figure 5O**, right panel). These results may indicate crosstalk between non-canonical Activin A signaling via Smad2, Smad1/5/8 and MEK/ERK pathways.

ACVRIB expression decreases across tumor stage in human HNSCC samples

To examine the expression level of ACVRIB expression for a utility as a diagnostic tool or stage-specific biomarker, we stained a commercially available tissue microarray (TMA) containing 72 normal and HNSCC tissues with antibodies against ACVRIB, ActRIIB, and ActA. Interestingly, we found that positive ACVRIB staining area was significantly decreased in the HNSCC samples compared to the normal controls (**Figure 6A**). As the control sections of the TMA were from normal tongue, we next wanted to compare the normal controls and the tongue SCC with SCCs from other sites and found that ACVRIB expression was decreased in both

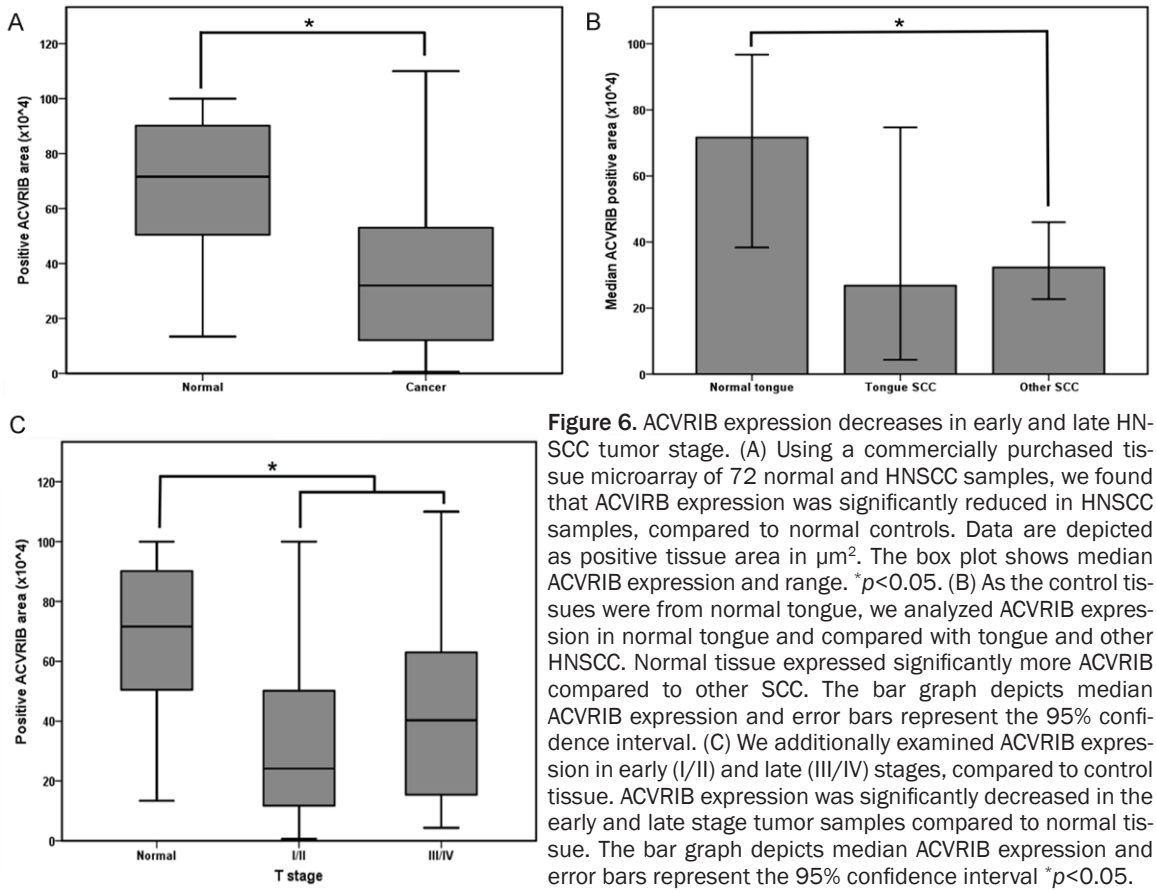

Figure 6. ACVRIB expression decreases in early and late HNSCC tumor stage. (A) Using a commercially purchased tissue microarray of 72 normal and HNSCC samples, we found that ACVIRB expression was significantly reduced in HNSCC samples, compared to normal controls. Data are depicted as positive tissue area in μm^2. The box plot shows median ACVRIB expression and range. $^*p<0.05$. (B) As the control tissues were from normal tongue, we analyzed ACVRIB expression in normal tongue and compared with tongue and other HNSCC. Normal tissue expressed significantly more ACVRIB compared to other SCC. The bar graph depicts median ACVRIB expression and error bars represent the 95% confidence interval. (C) We additionally examined ACVRIB expression in early (I/II) and late (III/IV) stages, compared to control tissue. ACVRIB expression was significantly decreased in the early and late stage tumor samples compared to normal tissue. The bar graph depicts median ACVRIB expression and error bars represent the 95% confidence interval $^*p<0.05$.

tongue and other SCCs compared to normal tongue controls; thereby, establishing that decreased ACVRIB expression is consistent across HNSCC (**Figure 6B**). Next, we assessed the relationship of ACVRIB between early (I/II) and late (III/IV). We found that ACVRIB is consistently decreased in early and late stages compared to normal controls (**Figure 6C**). We additionally examined ActRIIB and Activin A expression in early and late stage, compared to control, and found a non-significant decrease and increase, respectively (Supplemental Figure 4A, 4B).

Discussion

In the current study, we characterized the functional consequences of ACVRIB loss in HNSCC and ESCC. The Activin A signaling cascade has been long studied for its critical role in development across species [43, 44], however its actions in cancer have been widely disputed as the functions of Activin A appear to be almost entirely cell-type and context dependent [45]. To better explore the impact of this pathway in HNSCC and ESCC, we focused on ACVRIB, as we had previous described the inverse correlation between Activin A (*INHBA*) and ACVRIB expression in advanced ESCC [3]. We eliminated Activin A signaling via ACVRIB using CRISPR/Cas9-mediated knockout of ACVRIB, to discern the functional effects of loss of canonical Activin A signaling. Loss of canonical Activin A signaling mediated by ACVRIB results in increased proliferation, migration, and invasion.

We observed that ACVRIB-KO cells have the ability to simultaneously proliferate and invade in three-dimensional OTC. The relationship between proliferation and invasion of cancer cells has been debated, as it has been suggested that cells that are proliferating are not actively invading, and vice versa [46]. Though the leading hypothesis is that proliferation and invasion are mutually exclusive processes, several reports have suggested that this may not be the case. Tumuluri *et al.* and Dissanayake *et al.* found that OSCC patient tissues had an

increased proliferation index, as indicated by Ki67 staining, along the invasive front of the tumor tissue [47, 48]. Our data indicates a similar phenomenon: HNSCC cells at the leading edge both proliferate and invade in the absence of ACVRIB. Combined with the *in vitro* data, which showed an increased number of ACVRIB-KO cells in S and G2/M, this suggests that highly proliferative cells can also be responsible for the cancer cell invasion.

There is precedence for receptors of the TGFβ family to function in the maintenance of epithelial homeostasis. However, among the Activin type I receptors, little is noted regarding their downregulation or absence in cancer [1]. ACVRIB is among the most highly studied in terms of Activin type I receptors in cancer, however it remains unknown where loss of ACVRIB occurs: genomic, RNA, or protein level. The ESCC cell line TE-11 lacks ACVRIB protein but expresses *ACVRIB* mRNA ([3], data not shown). Therefore, further examination of the mechanism of ACVRIB regulation is needed, particularly in HNSCC and ESCC, as majority of the evidence regarding ACVRIB loss resides in other cancers.

Targeting ACVRIB *in vitro*, however, remains a challenge. Due to similarities between the ALKs, developing specific inhibitors for the individual family members is difficult [1]. In the current study, we treated SCC cells *in vitro* using the chemical inhibitor A83-01, which targets ALK 4/5/7. Because of the multifaceted effects of this inhibitor, we cannot say for certain that the phenotype we observed in OTC was solely the responsibility of ACVRIB inhibition. At this time, no inhibitors specifically target ALK4, as all available inhibitors also target other ALKs [1]. Therefore, using the CRISPR/Cas9 system demonstrated here is the closest to selectively targeting ACVRIB, though this is currently not feasible in the clinical context.

A main finding of this study was the regulation of the actin cytoskeleton and cell surface proteins by ACVRIB. Ultimately, dysregulation of ACVRIB expression and canonical Activin A signaling led to reorganization of the actin cytoskeleton and, thus, expression of cell surface proteins involved in cell-cell and cell-ECM interaction. In respect to ACVRIB, little to no evidence has been published exploring such functional effects and, therefore, we have established a novel role for this pathway. Some investigation, however, has described the actions of Activin A during some of these processes, though not in cancer. Riedy and colleagues described that stimulation of smooth muscle cells with Activin A led to migration and the formation of actin stress fibers and focal adhesions [49]. A similar effect was investigated in adipose stromal cells, Activin A could promote differentiation along the smooth muscle cell lineage. Treatment with an ALK 4/5/7 inhibitor could block such effects [50].

Though we have unearthed a new role for Activin A-ACVRIB signaling in HNSCC and ESCC, there remain many questions. We have just begun to scratch the surface of Activin A signaling in the absence of ACVRIB, potentially through an alternate Activin type I receptor. Therefore, further investigation into the mechanism of Activin A in this context is necessary to contribute to our deeper understanding of the pathway as well as potential ways to use this information for targeted therapeutics. If it is indeed the case that Activin A, working through an alternate pathway in the absence of ACVRIB, exerts oncogenic effects, the utilization of an Activin A ligand trap, such as follistatin, may aide in improving patient outcome in HNSCC and/or ESCC. In addition, attaining a better understanding of the role of the Activin A-ACVRIB interaction in a more complex physiological context, such as ACVRIB-KO cells in the presence of endothelial cells, immune cells, fibroblasts, neurons, etc., may provide a more complete understanding to how Activin A operates without epithelial expression of ACVRIB.

Despite the remaining questions surrounding the relationship between Activin A and ACVRIB, in this study we provided evidence showing the necessity of ACVRIB-dependent Activin A signaling in the regulation of HNSCC and ESCC. When this system becomes disrupted through downregulation of ACVRIB, HNSCC and ESCC become more aggressive. Clinically, this would ultimately lead to a worse prognosis for patients affected by this deletion. Therefore, further investigation into the consequences and potential therapeutic options revolving around Activin A-ACVRIB may promote better clinical outcomes in SCC.

Acknowledgements

This work was supported by grants from the National Institutes of Health (DK094900, DK-091491 to CDA; T32-CA0095193-26, F31-DE025477-01A1 to HAL; F31-CA189764 to KH; R01-CA1430815 to AZ), the Department of Veterans Affairs (VA CDA IK2BX002498 to SAA), and additional funding sources (AIHS 201201250, CRIO Project (Canada) to AZ). The use of Research Cores is supported by the Vanderbilt-Ingram Cancer Center (P30 CA68-4850 and the Vanderbilt Digestive Disease Research Center P30 DK058404 to CDA; VR-16470 to HAL; CTSA UL1-TR000445 to SAA; VUMC 53530, 53783, 44192-R, 61087 to AZ). The VMC Flow Cytometry Shared Resource is supported by the Vanderbilt Ingram Cancer Center (P30 CA68485) and the Vanderbilt Digestive Disease Research Center (DK05-8404). We would like to thank the Beauchamp, Belkhiri, El-Rifai, Zaika, and Zijlstra laboratories for their support and suggestions during the development, execution, and analysis of this project. We would also like to thank Dr. Anna Means, Christy Nichols, Christy Hinkle, Dianne Mason, Phil Williams and the Vanderbilt University Medical Center Section of Surgical Sciences for their additional support. Finally, we would like to thank David Flaherty, Brittany Matlock, and Christian Warren for their assistance in performing flow cytometry sorts and cell cycle analysis.

Disclosure of conflict of interest

None.

Abbreviations

ActRII, Activin receptor type II; ActRIIB, Activin receptor type IIB; ACVRIB, Activin receptor IB; ALK, Activin receptor-like kinase; ECM, extracellular matrix; EdU, 05-ethynyl-2'-deoxyuridine; ESCC, esophageal squamous cell carcinoma; FST, follistatin; GDF, growth and differentiation factors; HNSCC, head and neck squamous cell carcinoma; K13, cytokeratin 13; K19, cytokeratin 19; MAts, magnetically attachable stencils; OSCC, oral squamous cell carcinoma; PI, propridium iodide; SCC, squamous cell carcinoma.

Address correspondence to: Claudia D Andl, Burnett School of Biomedical Sciences, College of Medicine, University of Central Florida, 4110 Libra Dr. Bldg 20, BMS 223 Orlando, FL 32816, USA. E-mail: claudia.andl@ucf.edu

References

[1] Loomans HA, Andl CD. Activin receptor-like kinases: a diverse family playing an important role in cancer. Am J Cancer Res 2016; 6: 2431-2447.

[2] Heldin CH, Landström M, Moustakas A. Mechanism of TGF-β signaling to growth arrest, apoptosis, and epithelial-mesenchymal transition. Curr Opin Cell Biol 2009; 21: 166-176.

[3] Loomans HA, Arnold SA, Quast LL, Andl CD. Esophageal squamous cell carcinoma invasion is inhibited by Activin A in ACVRIB-positive cells. BMC Cancer 2016; 16: 873.

[4] Salogni L, Musso T, Bosisio D, Mirolo M, Jala VR, Haribabu B, Locati M, Sozzani S. Activin A induces dendritic cell migration through the polarized release of CXC chemokine ligands 12 and 14. Blood 2009; 113: 5848-5856.

[5] Zhang L, Deng M, Parthasarathy R, Wang L, Mongan M, Molkentin JD, Zheng Y, Xia Y. MEKK1 transduces activin signals in keratinocytes to induce actin stress fiber formation and migration. Mol Cell Biol 2005; 25: 60-65.

[6] Armes NA, Smith JC. The ALK-2 and ALK-4 activin receptors transduce distinct mesoderm-inducing signals during early Xenopus development but do not co-operate to establish thresholds. Development 1997; 124: 3797-3804.

[7] Pomeraniec L, Hector-Greene M, Ehrlich M, Blobe GC, Henis YI. Regulation of TGF-β receptor hetero-oligomerization and signaling by endoglin. Mol Biol Cell 2015; 26: 3117-3127.

[8] Romano V, Raimondo D, Calvanese L, D'Auria G, Tramontano A, Falcigno L. Toward a better understanding of the interaction between TGF-β family members and their ALK receptors. J Mol Model 2012; 18: 3617-3625.

[9] Attisano L, Wrana JL, Cheifetz S, Massagué J. Novel activin receptors: distinct genes and alternative mRNA splicing generate a repertoire of serine/threonine kinase receptors. Cell 1992; 68: 97-108.

[10] Gu Z, Nomura M, Simpson BB, Lei H, Feijen A, van den Eijnden-van Raaij J, Donahoe PK, Li E. The type I activin receptor ActRIB is required for egg cylinder organization and gastrulation in the mouse. Genes Dev 1998; 12; 844-857.

[11] Qiu W, Li X, Tang H, Huang AS, Panteleyev AA, Owens DM, Su GH. Conditional activin receptor type 1B (Acvr1b) knockout mice reveal hair loss abnormality. J Invest Dermatol 2010; 131; 1067-1076.

[12] Alexander JM, Bikkal HA, Zervas NT, Laws ER, Klibanski A. Tumor-specific expression and alternate splicing of messenger ribonucleic acid encoding activin/transforming growth factor-β receptors in human pituitary adenomas. J Clin Endocrinol Metab 1996; 81: 783-790.

[13] Danila DC, Zhang X, Zhou Y, Haidar JN, Klibanski A. Overexpression of wild-type activin receptor Alk4-1 restores Activin Antiproliferative effects in human pituitary tumor cells. J Clin Endocrinol Metab 2002; 87: 4741-4746.
[14] Su GH, Bansal R, Murphy KM, Montgomery E, Yeo CJ, Hruban RH, Kern SE. ACVR1B (ALK4, activin receptor type 1B) gene mutations in pancreatic carcinoma. Proc Natl Acad Sci U S A 2001; 98: 3254-7.
[15] Murphy KM, Brune KA, Griffin C, Sollenberger JE, Petersen GM, Bansal R, Hruban RH, Kern SE. Evaluation of candidate genes MAP2K4, MADH4, ACVR1B, and BRCA2 in familial pancreatic cancer: deleterious BRCA2 mutations in 17%. Cancer Res 2002; 62: 3789-3793.
[16] Kandoth C, McLellan MD, Vandin F, Ye K, Niu B, Lu C, Xie M, Zhang Q, McMichael JF, Wyczalkowski MA, Leiserson MDM, Miller CA, Welch JS, Walter MJ, Wendl MC, Ley TJ, Wilson RK, Raphael BJ, Ding L. Mutational landscape and significance across 12 major cancer types. Nature 2013; 502: 333-339.
[17] Kashyap MK, Pawar HA, Keerthikumar S, Sharma J, Goel R, Mahmood R, Kumar MV, Kumar KV, Pandey A, Kumar RV, Prasad TS, Harsha HC. Evaluation of protein expression pattern of stanniocalcin 2, insulin-like growth factor-binding protein 7, inhibin beta a and four and a half LIM domains 1 in esophageal squamous cell carcinoma. Cancer Biomark 2013; 12: 1-9.
[18] Kelner N, Rodrigues PC, Bufalino A, Fonseca FP, Santos-Silva AR, Miguel MC, Pinto CA, Leme AF, Graner E, Salo T, Kowalski LP, Coletta RD. Activin A immunoexpression as predictor of occult lymph node metastasis and overall survival in oral tongue squamous cell carcinoma. Head Neck 2015; 37: 479-486.
[19] Yoshinaga K, Inoue H, Utsunomiya T, Sonoda H, Masuda T, Mimori K, Tanaka Y, Mori M. N-cadherin is regulated by Activin A and associated with tumor aggressiveness in esophageal carcinoma. Clin Cancer Res 2004; 10: 5702-5707.
[20] Ashby WJ, Wikswo JP, Zijlstra A. Magnetically attachable stencils and the non-destructive analysis of the contribution made by the underlying matrix to cell migration. Biomaterials 2012; 33: 8189-8203.
[21] Shrivastava S, Steele R, Sowadski M, Crawford SE, Varvares M, Ray RB. Identification of molecular signature of head and neck cancer stem-like cells. Sci Rep 2015; 5: 1-8.
[22] Schindelin J, Arganda-Carreras I, Frise E, Kaynig V, Longair M, Pietzsch T, Preibisch S, Rueden C, Saalfeld S, Schmid B, Tinevez JY, White DJ, Hartenstein V, Eliceri K, Tomancak P, Cardona A. Fiji: an open-source platform for biological-image analysis. Nat Meth 2012; 9: 676-682.
[23] Le Bras GF, Loomans HA, Taylor CJ, Revetta FL, Andl CD. Activin A balance regulates epithelial invasiveness and tumorigenesis. Lab Invest 2014; 94: 1-13.
[24] Hahn SA, Schutte M, Hoque AT, Moskaluk CA, da Costa LT, Rozenbaum E, Weinstein CL, Fischer A, Yeo CJ, Hruban RH, Kern SE. DPC4, a candidate tumor suppressor gene at human chromosome 18q21.1. Science 1996; 271: 350-353.
[25] Zhou Y, Sun H, Danila DC, Johnson SR, Sigai DP, Zhang X, Klibanski A. Truncated activin type I receptor Alk4 isoforms are dominant negative receptors inhibiting activin signaling. Mol Endocrinol 2000; 14: 2066-2075.
[26] Alves RD, Eijken M, Bezstarosti K, Demmers JA, van Leeuwen JP. Activin A suppresses osteoblast mineralization capacity by altering extracellular matrix (ECM) composition and impairing matrix vesicle (MV) production. Mol Cell Proteomics 2013; 12: 2890-2900.
[27] Yoshinaga K, Yamashita K, Mimori K, Tanaka F, Inoue H, Mori M. Activin A causes cancer cell aggressiveness in esophageal squamous cell carcinoma cells. Ann Surg Oncol 2007; 15: 96-103.
[28] Bremnes RM, Donne T, Al-Saad S, Al-Shibli K, Andersen S, Sirera R, Camps C, Marinez I, Busund LT. The role of tumor stroma in cancer progression and prognosis: emphasis on carcinoma-associated fibroblasts and non-small cell lung cancer. J Thorac Oncol 2011; 6: 209-217.
[29] Nair KS. Expression of cell adhesion molecules in oesophageal carcinoma and its prognostic value. J Clin Pathol 2005; 58: 343-351.
[30] de Moraes FP, Lourenço SV, Ianez RC, de Sousa EA, Silva MM, Damascena AS, Kowalski LP, Soares FA, Coutinho-Camillo CM. Expression of stem cell markers in oral cavity and oropharynx squamous cell carcinoma. Oral Surg Oral Med Oral Pathol Oral Radiol 2017; 123: 113-122.
[31] Stojanović N, Brozovic A, Majhen D, Bosnar MH, Fritz G, Osmak M, Ambriovic-Ristov A. Integrin αvβ3 expression in tongue squamous carcinoma cells Cal27 confers anticancer drug resistance through loss of pSrc(Y418). Biochim Biophys Acta 2016; 1863: 1969-1978.
[32] Gomez-Lamarca MJ, Cobreros-Reguera L, Ibanez-Jimenez B, Palacios IM, Martin-Bermudo MD. Integrins regulate epithelial cell differentiation by modulating notch activity. J Cell Science 2014; 127: 4667-4678.
[33] Lee JL, Steuli CH. Commentary: integrins and epithelial cell polarity. J Cell Science 2014; 127: 3199-3204.
[34] Kim KH, Kim L, Choi SJ, Han JY, Kim JM, Chu YC, Kim YM, Park IS, Lim JH. The clinicopatho-

logical significance of epithelial mesenchymal transition associated protein expression in head and neck squamous cell carcinoma. Korean J Pathol 2014; 48: 263-7.
[35] Hu J, Wang X, Wei SM, Tang YH, Zhou Q, Huang CX. Activin A stimulates the proliferation and differentiation of cardiac fibroblasts via the ERK1/2 and p38-MAPK pathways. Eur J Pharmacol 2016; 789: 319-327.
[36] Andl CD, Fargnoli BB, Okawa T, Bowser M, Takaoka M, Nakagawa H, Klein-Szanto A, Hua X, Herlyn M, Rustgi A. Coordinated functions of E-cadherin and transforming growth factor β receptor II in vitro and in vivo. Cancer Res 2006; 66: 9878-9885.
[37] Ida-Yonemochi H, Maruyama S, Kobayashi T, Yamazaki M, Cheng J, Saku T. Loss of keratin 13 in oral carcinoma in situ: a comparative study of protein and gene expression levels using paraffin sections. Modern Pathol 2012; 25: 784-794.
[38] Zhong LP, Zhang CP, Zheng JW, Li J, Chen WT, Zhang ZY. Increased Cyfra 21-1 concentration in saliva from primary oral squamous cell carcinoma patients. Arch Oral Biol 2007; 52: 1079-1087.
[39] Martins da Silva SJ, Bayne RA, Cambray N, Hartley PS, McNeilly AS, Anderson RA. Expression of activin subunits and receptors in the developing human ovary: Activin A promotes germ cell survival and proliferation before primordial follicle formation. Dev Biol 2004; 266: 334-345.
[40] Neely MD, Litt MJ, Tidball AM, Li GG, Aboud AA, Hopkin CR, Chamberlin R, Hong CC, Ess KC, Bowman AB. DMH1, a highly selective small molecule BMP inhibitor promotes neurogenesis of hiPSCs: comparison of PAX6 and SOX1 expression during neural induction. ACS Chem Neurosci 2012; 3: 482-491.
[41] Tojo M, Hamashima Y, Hanyu A, Kajimoto T, Saitoh M, Miyazono K, Node M, Imamura T. The ALK-5 inhibitor A-83-01 inhibits Smad signaling and epithelial-to-mesenchymal transition by transforming growth factor-β. Cancer Science 2005; 96: 791-800.
[42] Ashida Y, Nakajima-Koyama M, Hirota A, Yamamoto T, Nishida E. Activin A in combination with ERK1/2 MAPK pathway inhibition sustains propagation of mouse embryonic stem cells. Genes Cells 2017; 22: 189-202.
[43] Sui L, Bouwens L, Mfopou JK. Signaling pathways during maintenance and definitive endoderm differentiation of embryonic stem cells. Int J Dev Biol 2013; 57: 1-12.
[44] Wijayarathna R, de Kretser DM. Activins in reproductive biology and beyond. Hum Reprod Update 2016; 22: 342-357.
[45] Loomans H, Andl C. Intertwining of Activin A and TGFβ signaling: dual roles in cancer progression and cancer cell invasion. Cancers 2015; 7: 70-91.
[46] Kohrman AQ, Matus DQ. Divide or conquer: cell cycle regulation of invasive behavior. Trends Cell Biol 2017; 27: 12-25.
[47] Tumuluri V, Thomas GA, Fraser IS. The relationship of proliferating cell density at the invasive tumour front with prognostic and risk factors in human oral squamous cell carcinoma. J Oral Pathol Med 2004; 33: 204-208.
[48] Dissanayake U, Johnson NW, Warnakulasuriya KA. Comparison of cell proliferation in the centre and advancing fronts of oral squamous cell carcinomas using Ki-67 index. Cell Prolif 2003; 36: 255-264.
[49] Riedy MC, Brown MC, Molloy CJ, Turner CE. Activin A and TGF-β stimulate phosphorylation of focal adhesion proteins and cytoskeletal reorganization in rat aortic smooth muscle cells. Exp Cell Res 1999; 251: 194-202.
[50] Merfeld-Clauss, S, Lupov IP, Lu H, Feng D, Compton-Craig P, March KL, Trakuev DO. Adipose stromal cells differentiate along a smooth muscle lineage pathway upon endothelial cell contact via induction of Activin A. Circ Res 2014; 115: 800-809.

Supplemental Table 1. Antibodies used for FFPE immunofluorescence

Antibody	Dilution	Vendor
ACVRIB	1:200	Abcam
α2 integrin	1:200	BD Biosciences
α5 integrin	1:200	BD Biosciences
αv integrin	1:200	BD Biosciences
β1 integrin	1:200	BD Biosciences
β3 integrin	1:200	BD Biosciences
β4 integrin	1:200	BD Biosciences
Ki67	1:200	Cell Signal Technology
E-cadherin	1:200	BD Biosciences
Vimentin	1:200	Cell Signal Technology
Cytokeratin 13 (K13)	1:200	Abcam
Cytokeratin 19 (K19)	1:200	Abcam

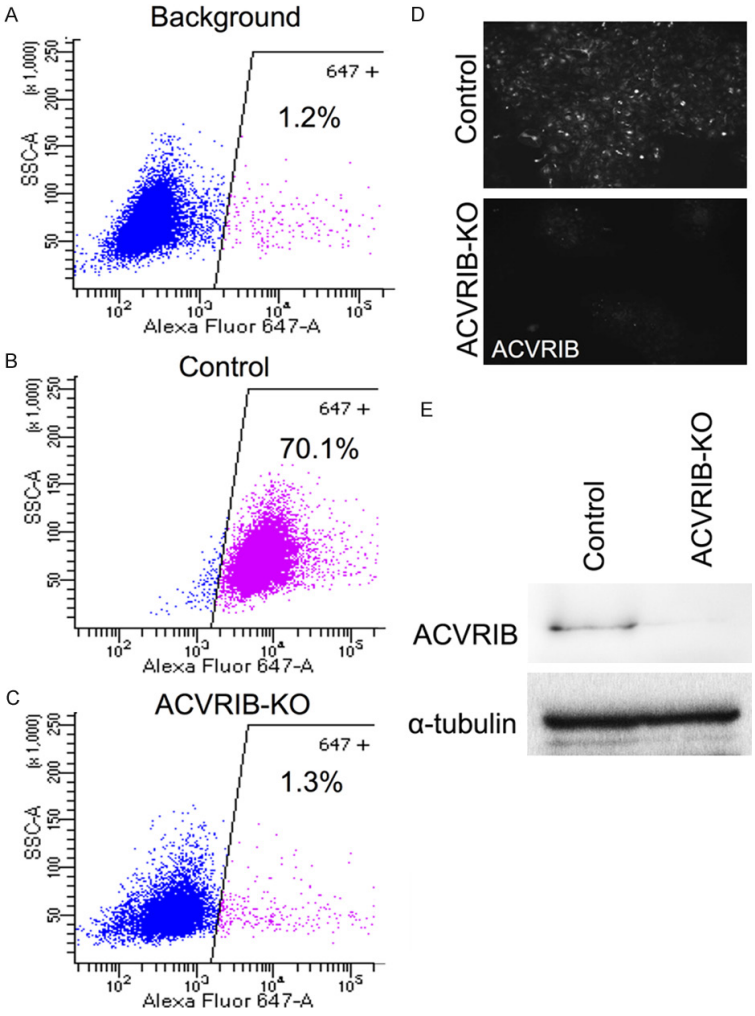

Supplemental Figure 1. Validation of ACVRIB knockout in OSC-19 head and neck squamous cells. Cells were validated by several methods. Flow cytometry showing (A) background stain (B) control and (C) ACVRIB-KO populations. (D) Immunofluorscence staining of ACVRIB in control (top) and ACVRIB-KO (bottom) cells. (E) Western blot of control and ACVRIB-KO OSC-19 cells. α-tubulin was used as a loading control.

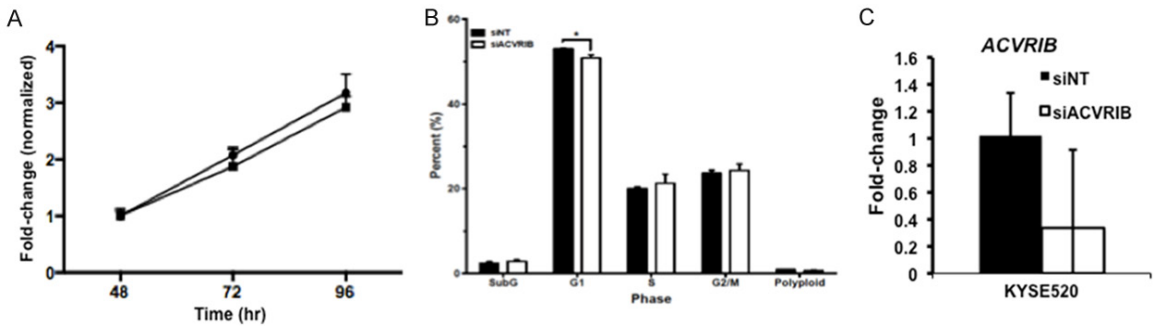

Supplemental Figure 2. Proliferation assays of KYSE520 cells. A. Cell counting, beginning 48 hours after transfection, revealed no differences in proliferation between siNT and siACVRIB knockdown cells. B. siACVRIB cells had significantly less cells in G1, and more cells in S and G2/M, though not statistically significant. C. qRT-PCR of ACVRIB in KYSE520.

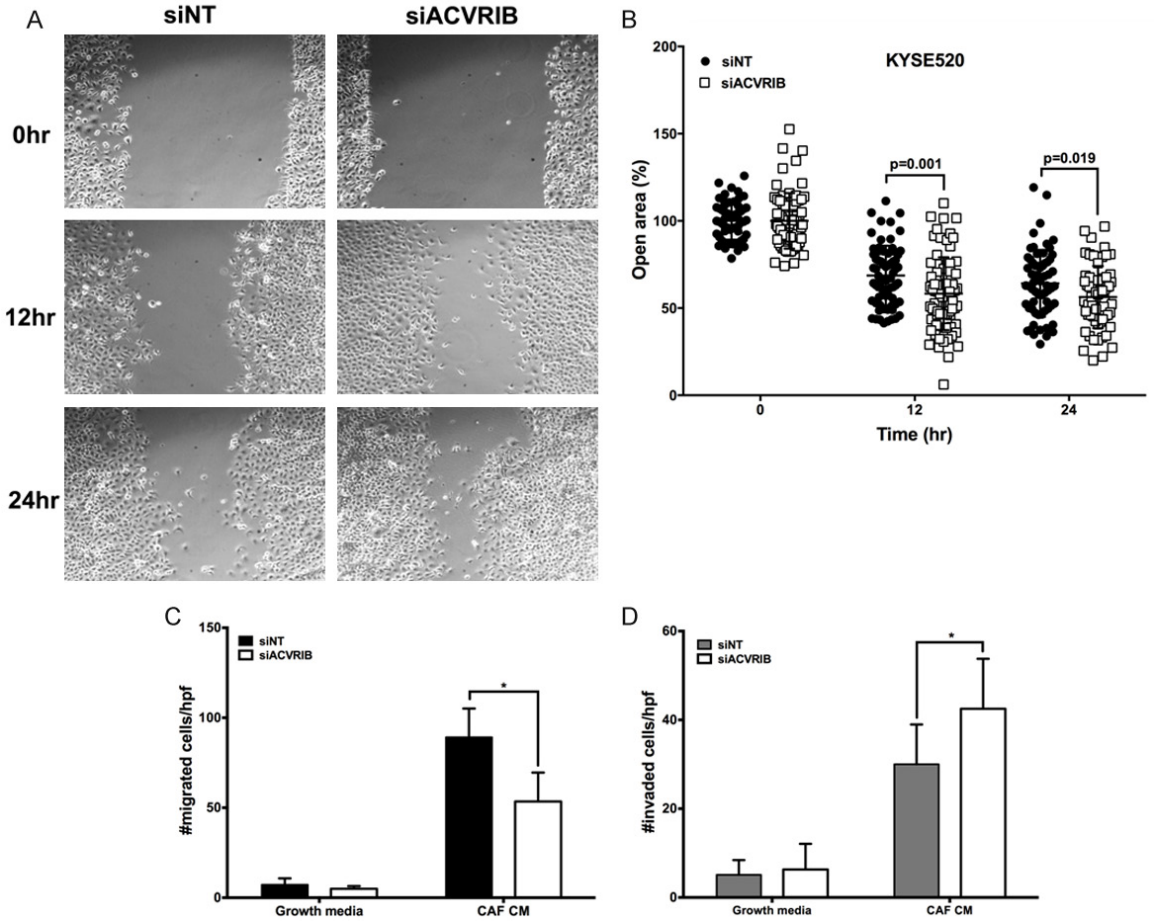

Supplemental Figure 3. Knockdown of ACVRIB by siRNA in KYSE520 enhances directional motility. (A) By 12 hours and 24 hours, siACVRIB knockdown cells close more open MAts area than non-targeting control (siNT). (B) Quantification of MAts assay shown in (A). (C) Quantification of number of migrated KYSE520 siACVRIB or siNT cells per high-powered field (hpf). Cells were stained with 0.1% crystal violet and counted. There were less KYSE520 siACVRIB cells that migrated through the Boyden chamber cmpared to siNT. (D) Similar to (C), quantification of number of invaded KYSE520 cells per high powered field. KYSE520 siACVRIB cells invaded more in Boyden chamber assay than siNT. *$p<0.05$.

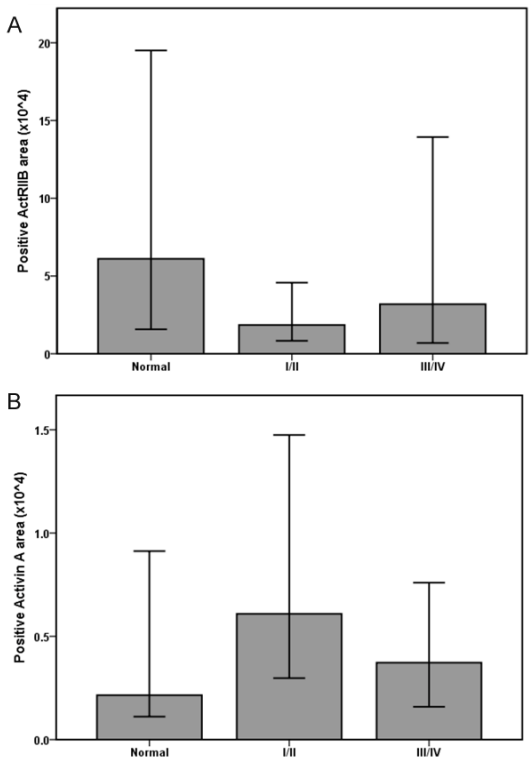

Supplemental Figure 4. ActRIIB and Activin A expression in early (I/II) and late (III/IV) stage HNSCC. A. Compared to controls, ActRIIB expression was non-significantly decreased in early (I/II) and late (III/IV) stage HNSCC tumor samples. B. Conversely, Activin A expression was non-significantly increased in early (I/II) and late (III/IV) stage HNSCC samples compared to normal tissue. The bar graphs depict median ActRIIB and Activin A expression and error bars represent the 95% confidence interval.